Proc. Natl. Acad. Sci. USA
Vol. 80, pp. 6513–6517, November 1983
Biochemistry

Polymerization of actin: Mechanism of the Mg^{2+}-induced process at pH 8 and 20°C

(metal binding/conformational change/nucleation)

CARL FRIEDEN

Department of Biological Chemistry, Division of Biology and Biomedical Sciences, Washington University School of Medicine, St. Louis, MO 63110

Communicated by David M. Kipnis, July 25, 1983

ABSTRACT **A detailed mechanism that fully accounts for the Mg^{2+}-induced polymerization of actin in the presence or absence of Ca^{2+} at 20°C and pH 8 is presented. In the absence of Ca^{2+}, the mechanism of the Mg^{2+}-induced polymerization is as follows: Mg^{2+} binds to a metal-binding site on G-actin and induces a conformational change, which is required for eventual polymerization. The overall dissociation constant for this binding is about 30 μM. This actin species then binds a second molecule of Mg^{2+} (K_d = 5 mM), which yields a species capable of polymerization. Dimer formation from this monomeric species is quite unfavorable, but trimer formation from dimer and monomer is much more favorable. The trimer may then elongate to give filaments. Ca^{2+}, when present, binds at the same site as the tightly bound Mg^{2+} and must be displaced by Mg^{2+} before the conformational change can occur. The rate and dissociation constants for tight binding of Ca^{2+} and Mg^{2+} and for the conformational change are consistent with those observed previously by using a fluorescently labeled G-actin. With the mechanism proposed, it is possible to fit the full time course of polymerization over a wide range of actin concentrations, Mg^{2+} concentrations, and Ca^{2+} concentrations.**

Actin polymerization induced by Mg^{2+} has been presumed to be a nucleation–elongation process (1–3). It has been shown previously, however, that when Mg^{2+} binds to monomeric G-actin it induces a conformational change (4, 5), and recent evidence suggests that, with Mg^{2+}, an activation step is required prior to polymerization (6–8). The present paper confirms this observation and shows that the conformational change induced by Mg^{2+} in G-actin that was previously observed (4, 5) is the same as that required for the polymerization process. Thus the simple nucleation–elongation model is not sufficient to describe the Mg^{2+}-induced polymerization. However, Mg^{2+} binding to this site is not the major controlling factor in the polymerization. Rather, Mg^{2+} binding to a site of lower affinity is required. There is evidence for low-affinity Mg^{2+}-binding sites (9, 10), but it has never been clear what the dissociation constant is or how many Mg^{2+}-binding sites are required to explain the rate dependence. The present paper suggests that only a single low-affinity site (K_d = 5 mM) is required.

Although the nucleation–elongation process subsequent to Mg^{2+} binding is the model used, there has been disagreement about the size of the nucleus, with values ranging from two to four monomer units (6, 7, 11, 12). Because of the nature of the equations that describe the polymerization process, investigators have had to assume that formation of each species prior to that of the nucleus that undergoes elongation is equally unfavorable. This paper describes the time course of polymerization by using a computer simulation system in which the assumption is not a necessary one. The data suggest that, although the species that elongates is indeed a trimer, the formation of trimer is much more favorable than the formation of dimer. I provide here a mechanism that quantitatively describes the full time course of actin polymerization as a function of actin concentration, Mg^{2+} concentration, and Ca^{2+} concentration.

MATERIALS AND METHODS

Actin. Rabbit skeletal muscle G-actin was isolated and purified according to Spudich and Watt (13) with gel filtration (Sephadex G-150) as described (14). Unless used immediately after gel filtration, actin was stored at −20°C after lyophilization in the presence of sucrose (2 mg per mg of actin). Lyophilized actin was dialyzed at 4°C for 1–2 days either against 2 mM Tris·HCl, pH 8/200 μM ATP/200 μM $CaCl_2$/1.5 mM NaN_3 or against 2 mM Tris·HCl, pH 8/100 μM ATP/50 μM $MgSO_4$/1.5 mM NaN_3/200 μM dithiothreitol for Ca^{2+}-free actin (6). The protein concentration was determined spectrophotometrically by using a value of $A^{1\,mg/ml} = 0.63$ at 290 nm (15) or by Bradford determination (16) for pyrene-labeled actin with G-actin as a standard.

Polymerization Kinetics. All actin solutions were centrifuged before use at 180,000 × *g* for 30 min or 100,000 × *g* for 60 min. The polymerization process was followed continuously by fluorescence, using trace amounts of pyrene-labeled actin (excitation 365 nm, emission 386 nm) as described (17). Because the fluorescence change (≈25-fold) on polymerization is independent of the pyrene-labeled actin concentration (17), the amount of pyrene-labeled actin was kept constant (≈5 μg/ml) even in experiments in which the total actin concentration was changed. The advantages of this assay for quantitative measurement of actin polymerization have been discussed elsewhere (6, 7, 17). Solutions were stirred with a magnetic stirrer in the bottom of the fluorescence cuvette for only 10 sec after addition of the amount of Mg^{2+} required to start the polymerization. All polymerization reactions were performed at 20°C. Data were stored in a mode that could be used as a real data curve in the simulation program described below.

Simulation of the Full Time Course. A general system of computer simulation of kinetic mechanisms by numerical integration has been described (18). It is possible to simulate actin polymerization (incorporation of monomer into polymer) by using this system and a mechanism of the type

$$\begin{aligned} A + A &\rightleftharpoons A_2 \\ A_2 + A &\rightleftharpoons A_3 \\ A_3 + A &\rightleftharpoons A_4 \\ &\vdots \\ A_6 + A &\rightleftharpoons A_n \\ A_n + A &\rightleftharpoons A_n \end{aligned} \qquad [1]$$

The publication costs of this article were defrayed in part by page charge payment. This article must therefore be hereby marked "*advertisement*" in accordance with 18 U.S.C. §1734 solely to indicate this fact.

Abbreviation: AEDANS-labeled G-actin, actin labeled with *N*-iodoacetyl-*N'*-(5-sulfo-1-naphthyl)ethylenediamine.

where A_n represents all polymers, and polymer formation is the difference between the total actin concentration and the concentration of those species prior to the polymer species A_n. When expressed in terms of monomer, polymer formation is $A_{total} - \Sigma_{i=2}^{5} iA_i$. The second term of this equation represents the concentration of dimer, trimer, etc., and these concentrations are normally quite small. The use of this system will be described more completely elsewhere (19). Scheme I represents an extension of this mechanism in terms of Ca^{2+} and Mg^{2+} binding prior to polymerization. Data are fit by visual inspection of real and simulated data as shown by the figures.

RESULTS

The mechanism for Mg^{2+}-induced polymerization of actin is shown in Scheme I.

$$1.\quad A + Ca \overset{K_{Ca}}{\rightleftharpoons} ACa$$

$$2.\quad A + Mg \overset{K_{Mg}}{\rightleftharpoons} AMg \overset{k_1}{\underset{k_{-1}}{\rightleftharpoons}} A'Mg$$

$$3.\quad A'Mg + Mg \overset{K'_{Mg}}{\rightleftharpoons} A'(Mg)_2$$

$$4.\quad A'(Mg)_2 + A'(Mg)_2 \overset{k_2}{\underset{k_{-2}}{\rightleftharpoons}} [A'(Mg)_2]_2$$

$$5.\quad [A'(Mg)_2]_2 + A'(Mg)_2 \overset{k_3}{\underset{k_{-3}}{\rightleftharpoons}} [A'(Mg)_2]_3$$

$$6.\quad \left\{ \begin{array}{l} \vdots \\ [A'(Mg)_2]_n + A'(Mg)_2 \overset{k_e}{\underset{k_{-e}}{\rightleftharpoons}} [A'(Mg)_2]_n \end{array} \right.$$

Scheme I

where A is monomeric G-actin, ACa is G-actin containing bound Ca^{2+}, A'Mg is a conformationally altered form of G-actin, k_e and k_{-e} are the elongation and disassembly rate constants, and n, in terms of Eq. 1, is assumed to be 6. For n values of 6 or larger there are no observable differences in the simulated time course; values between 3 and 6 are slightly different from each other. Thus, 6 was chosen as an accurate representation for the simulation. Step 6 of Scheme I represents the elongation process. Points to note about this mechanism are (*i*) Ca^{2+} and Mg^{2+} compete for binding to the so-called tight metal-binding site of G-actin; (*ii*) the conformational change induced by Mg^{2+} is a required step for polymerization; and (*iii*) binding of a second mole of Mg^{2+} is also required prior to polymerization. Portions of this mechanism are examined below.

Steps 4–6. Ca^{2+}-free G-actin may be prepared by dialysis of G-actin against a buffer of 2 mM Tris·HCl/100 μM ATP/50 μM $MgSO_4$/1.5 mM NaN_3/200 μM dithiothreitol, pH 8 (6). Prior to polymerization, the monomeric G-actin was incubated for 5 min at a Mg^{2+} concentration of 350 μM to induce the conformational change of step 2 (see below). After this time, all the G-actin is in the form A'Mg (Scheme I, step 2). The concentration of Mg^{2+} used here was not sufficient to induce any polymerization during the incubation time. After incubation, the appropriate amount of Mg^{2+} was added to start polymerization. The time course of polymerization at one level of Mg^{2+} (2 mM) as a function of actin concentration is shown in Fig. 1. Attempts to fit these data with the simulation program consistently indicate a nucleus size between a dimer and a trimer. Thus a mechanism that uses a dimer as the nucleus gives too small a change in polymerization rate as a function of actin concentration, and a trimer mechanism gives a change that is too large. For example, ratios of half-times of polymerization using a dimer and trimer nucleus over a 6-fold concentration difference as measured by simulation of Scheme I are 15 and 38, respectively, whereas the ratio for the real data (Fig. 1) is 26. A similar observation has been made at every other level of Mg^{2+} tested (1.5 mM–4 mM, data not shown). As will be discussed elsewhere (19), there are at least two ways by which this result may occur for a simple nucleation–elongation mechanism; one involves fragmentation of the filaments (or fragmentation and annealing) and the other involves unequal dissociation constants for dimer and trimer formation. A mechanism including fragmentation and annealing does not fit the data well.

The data shown in Fig. 1 are fit with the assumption that dimer formation from monomer is a very unfavorable step, but trimer formation from dimer and monomer is not nearly so unfavorable. The dissociation constants for dimer and trimer formation differ by a factor of about 10^5. The values used for these dissociation constants are given in Table 1.

Steps 3–6. Fig. 2 shows the Mg^{2+} dependence of polymerization at a given actin concentration. As above, these experiments were performed in the absence of Ca^{2+} and with incubation with sufficient Mg^{2+} to induce the conformational change indicated in step 2 of Scheme I but not sufficient to induce polymerization. By using the mechanism so far proposed (unequal dissociation constants for dimer and trimer), it is possible to fit these data with a single weak binding site for Mg^{2+}, using steps 3–6 of Scheme I. The dissociation constant of Mg^{2+} for this site is 5 mM (Table 1).

Steps 1–6. Fig. 3 shows the dependence of the polymerization rate on the concentration of Ca^{2+} at a given concentration of Mg^{2+} and actin. These data show that increasing concentrations of Ca^{2+} increase the lag time of the reaction and decrease the rate of polymerization. The data were fit by using the values given above for steps 3–6 but including a binding site that can bind either Ca^{2+} or Mg^{2+}. Subsequent to weak Mg^{2+} binding a conformational change is induced that leads to tight Mg^{2+} binding. The binding of Mg^{2+} to this site is directly competitive with Ca^{2+}. It has previously been shown that these steps occur in G-actin (4, 5). The incorporation of this process into the mechanism shows that the Mg^{2+}-induced conformational change is a prerequisite for polymerization. Table 1 lists the values used to fit the data of Fig. 3. As discussed below, these values are essentially identical to those determined by a totally independent method [i.e., the Mg^{2+}-induced fluorescence change of AEDANS-labeled G-actin (5)].

DISCUSSION

The mechanism proposed in Scheme I quantitatively explains the dependence of the time course of polymerization on actin concentration, on Mg^{2+} concentration, and on Ca^{2+} concentration. The first step in the scheme is the displacement of Ca^{2+} by Mg^{2+} which, subsequent to binding, induces a conformational change in the actin that is a prerequisite for the Mg^{2+}-induced polymerization process.

The process shown in steps 1 and 2 of Scheme I has also been described by a different method (4, 5). The Mg^{2+}-induced fluorescence change in AEDANS-labeled G-actin showed that Ca^{2+} and Mg^{2+} compete for a single site and that Mg^{2+} induces a time-dependent change in the fluorescence of labeled G-actin that can be reversed by Ca^{2+} (4, 5). The observed time-dependent response was interpreted as weak binding of Mg^{2+} followed by a conformational change to give tighter Mg^{2+} binding. Dissociation constants for Ca^{2+} and Mg^{2+} as well as for the rate of the conformational change were determined from these

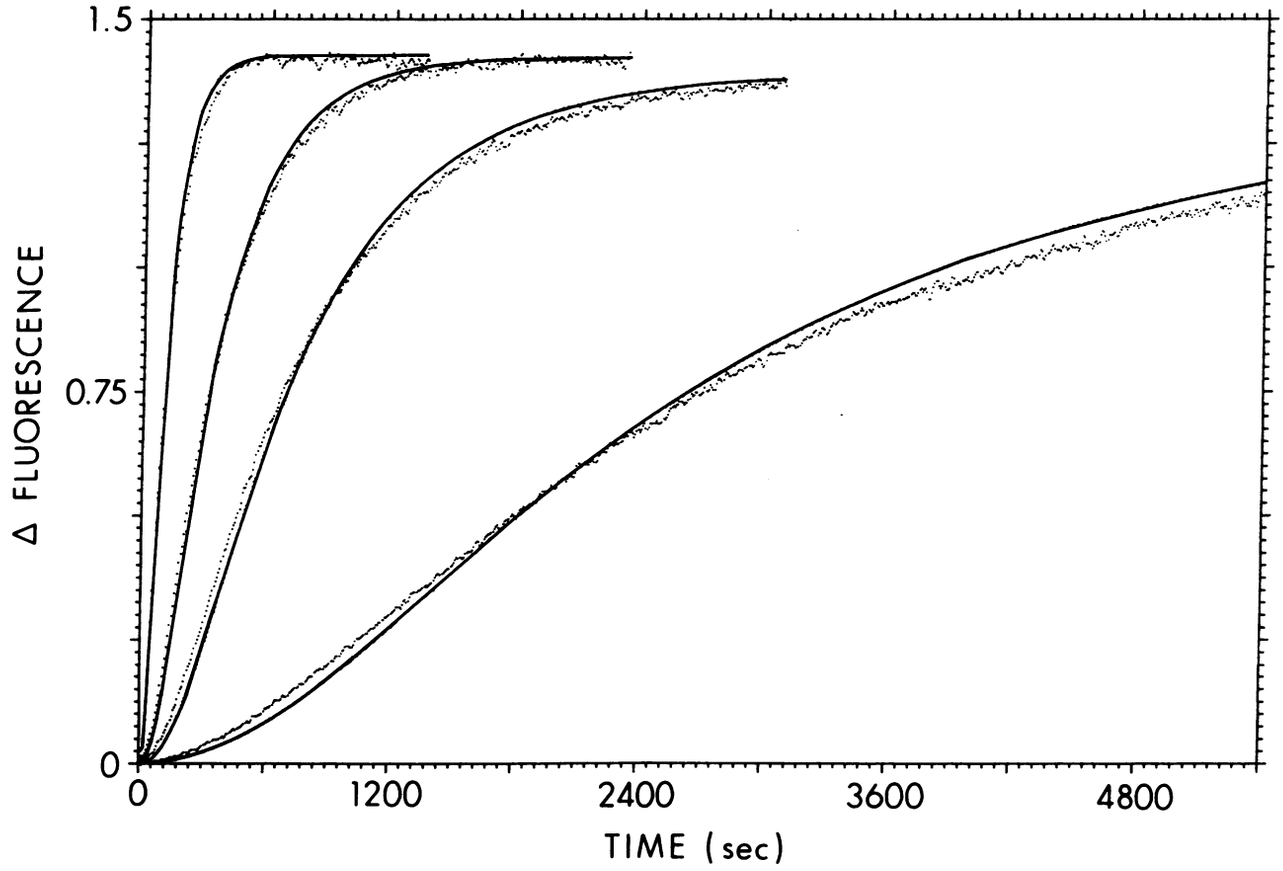

FIG. 1. Actin polymerization as a function of actin concentration. Polymerization was measured by the change in fluorescence of a constant trace amount of pyrene-labeled actin (17). Experimental conditions: 20°C, 2 mM Tris·HCl, pH 8/100 μM ATP/1.5 mM NaN_3. The actin was incubated for 5 min with 0.35 mM Mg^{2+} and then sufficient Mg^{2+} was added to make the final total concentration 2 mM. Actin concentrations used were (right to left) 5.87, 11.7, 17.6, and 35.2 μM. The solid lines are curves generated by computer simulation, using Scheme I and the kinetic parameters shown in Table 1.

experiments. These data are also shown in Table 1 and the agreement between the rate and dissociation constants from the two independent methods is so close as to be quite convincing that the changes observed with AEDANS-labeled G-actin are the same as those required for the polymerization. Recently, other investigators have also proposed a Mg^{2+}-induced activation step (6, 7), but they did not define the kinetic parameters associated with this step. I previously had also observed that displacement of Ca^{2+} with Mg^{2+} at this site leads to an increased off rate constant for the tightly bound ATP (5). Whether this is important in the polymerization process is unknown. The role of ATP hydrolysis in the polymerization process also remains unclear.

Table 1. Kinetic constants used to fit data according to Scheme I

Step	Constant*	Values obtained by using AEDANS-labeled G-actin (5)
1	$K_{Ca} = 20\ \mu M$	7 μM
2	$K_{Mg} = 900\ \mu M$	900 μM
	$k_1 = 0.33\ sec^{-1}$	$0.19\ sec^{-1}$
	$k_{-1} = 0.01\ sec^{-1}$	$0.01\ sec^{-1}$
	$K_{Mg}\ k_{-1}/k_1 = 27\ \mu M$	47 μM
3	$K'_{Mg} = 5$ mM	
4	$k_{-2}/k_2 = 8 \times 10^5\ \mu M$	
5	$k_{-3}/k_3 = 5\ \mu M$	
6	$k_{-e}/k_e = 0.15$†	

AEDANS, *N*-iodoacetyl-*N'*-(5-sulfo-1-naphthyl)ethylenediamine.

* For any given set of experiments, the same kinetic parameters were used. However, a variation of ±15% in values of k_{-2}/k_2 or k_{-3}/k_3 would have resulted in much better goodness-of-fit of the data within a given set.

† k_e was usually assumed to be $10^6\ mol^{-1}\ sec^{-1}$. When different batches of actin gave somewhat different rates of polymerization, the parameter varied was k_e and k_{-e}/k_e remained constant. It would have also been possible to change k_{-2} to account for these differences. In all cases, the maximum variation from different actin preparations was <2-fold. I did not test whether an additional polymerization–depolymerization cycle immediately prior to use would eliminate this variation.

The third step in Scheme I represents Mg^{2+} binding to a weak binding site. This binding is also required for polymerization and explains the Mg^{2+} dependence of the polymerization (Fig. 2). Other investigators have postulated weak binding Mg^{2+} sites to explain this dependence with the number of sites ranging from two to six (9, 10), but little data on the dissociation constant are available. It may be seen that only a single weak binding site with a dissociation constant of 5 mM is required to explain the data. Although it is possible that there are more weak binding sites, such sites would have to be independent and of equal affinity to yield the observed result. Because the data are explained in terms of a single low-affinity site, there is no reason to postulate multiple sites. There appears to be no time-dependent conformational change associated with this process, although if such a change were quite rapid it would not be observed.

The remaining steps of the scheme describe the polymerization process subsequent to the Mg^{2+} activation due to bind-

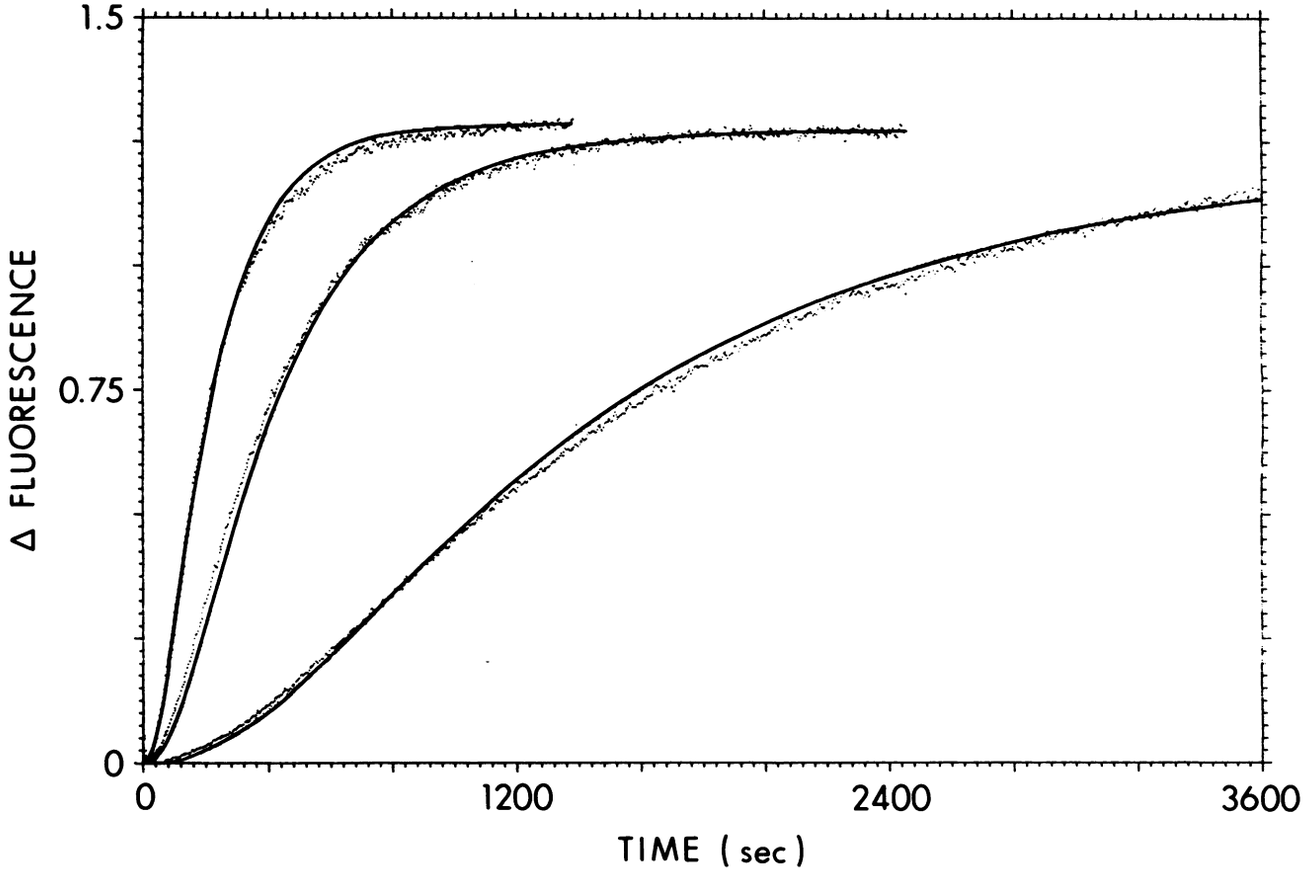

FIG. 2. Actin polymerization as a function of Mg^{2+} concentration. Experimental conditions are as described in the legend to Fig. 1. The actin concentration was 11.7 μM and the final total Mg^{2+} concentrations were (right to left) 1.5, 3.0, and 5.05 mM. The solid lines are curves generated by computer simulation, using Scheme I and the kinetic parameters shown in Table 1.

ing at the tight and weak binding sites. As noted above (see *Results*), the data are inconsistent with either a dimer or trimer as the nucleus but fall somewhere between these nucleus sizes. There may be more than one mechanism that could describe such results (19). However, the most likely explanation for such results is that dimer formation is much less favorable than trimer formation by several orders of magnitude. The data in Table 1 indicate a factor of about 10^5 difference in dimer and trimer formation.

It would appear from the constants chosen to describe the data that the critical concentration (k_{-e}/k_e) of actin under these conditions is 0.15 μM. This is somewhat lower than the observed values ($\approx$0.5 μM). However, an interesting aspect of the proposed mechanism is that the critical concentration shows some dependence on the Mg^{2+} concentration, because actin in the absence of 2 mol of Mg^{2+} is unable to polymerize. Thus the observed critical concentration will be somewhat higher than the ratio of rate constants for elongation and disassembly. For example, at 1, 2, and 4 mM Mg^{2+} the observed critical concentrations in the presence of 200 μM Ca^{2+}, using the kinetic parameters in Table 1, are 1.2, 0.6, and 0.36 μM, respectively, rather than the 0.15 μM expected from k_{-e}/k_e.

In summary, Mg^{2+}-induced actin polymerization has been described in quantitative terms. Essential for the polymerization is Mg^{2+} binding to a tight site (displacing any Ca^{2+} that may be there) and binding to a weak site. Dimer formation is much less favorable than trimer formation and elongation appears to proceed from the trimer. At 20°C and pH 8, the mechanism quantitatively describes data for the polymerization as a function of actin concentration, Mg^{2+} concentration, and Ca^{2+} concentration.

I thank Helen R. Gilbert for excellent technical assistance. This work was supported by Grant AM-13332 from the National Institutes of Health.

1. Oosawa, F. & Asakura, S. (1975) *Thermodynamics of the Polymerization of Protein* (Academic, New York).
2. Wegner, A. & Engel, J. (1975) *Biophys. Chem.* **3**, 215–225.
3. Korn, E. D. (1982) *Physiol. Rev.* **62**, 672–737.
4. Frieden, C., Lieberman, D. & Gilbert, H. R. (1980) *J. Biol. Chem.* **255**, 8991–8993.
5. Frieden, C. (1982) *J. Biol. Chem.* **257**, 2882–2886.
6. Tobacman, L. S. & Korn, E. D. (1983) *J. Biol. Chem.* **258**, 3207–3214.
7. Cooper, J. A., Buhle, E. L., Jr., Walker, S. B., Tsong, T. Y. & Pollard, T. D. (1983) *Biochemistry* **22**, 2193–2202.
8. Maruyama, K. (1981) *Biochim. Biophys. Acta* **667**, 139–142.
9. Martinosi, A., Molino, C. M. & Gergely, J. (1964) *J. Biol. Chem.* **239**, 1057–1064.
10. Rouayrenc, J. & Travers, F. (1981) *Eur. J. Biochem.* **116**, 73–77.
11. Wegner, A. & Savko, P. (1982) *Biochemistry* **21**, 1909–1913.
12. Wegner, A. (1982) *Nature (London)* **296**, 200–201.
13. Spudich, J. A. & Watt, S. (1971) *J. Biol. Chem.* **246**, 4866–4871.
14. MacLean-Fletcher, S. & Pollard, T. D. (1980) *Biochem. Biophys. Res. Commun.* **96**, 18–27.
15. Houk, T. W., Jr., & Ue, K. (1974) *Anal. Biochem.* **62**, 66–74.
16. Bradford, M. (1976) *Anal. Biochem.* **72**, 248–254.
17. Tellam, R. & Frieden, C. (1982) *Biochemistry* **21**, 3207–3214.
18. Barshop, B. A., Wrenn, R. F. & Frieden, C. (1983) *Anal. Biochem.* **130**, 134–145.
19. Frieden, C. & Goddette, D. W., *Biochemistry*, in press.

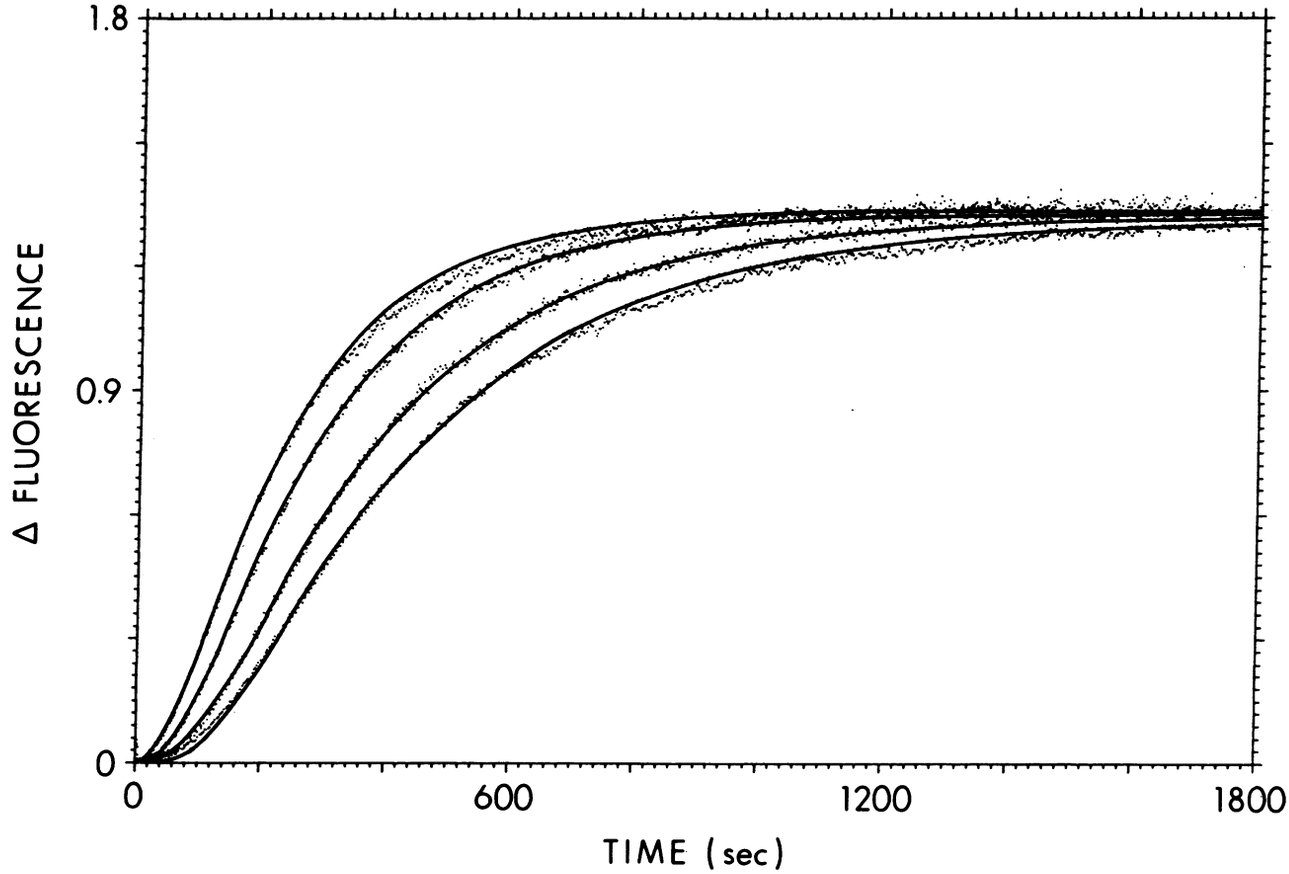

FIG. 3. Actin polymerization as a function of Ca^{2+} concentration. Experimental conditions are as described in the legend to Fig. 1. The Mg^{2+} concentration in all experiments was 4 mM and the actin concentration was 15.2 μM. The Ca^{2+} concentrations used were (left to right) 0, 100, 500, and 1,000 μM. G-actin was dialyzed overnight against buffer containing no Ca^{2+} and no Mg^{2+}. Ca^{2+} was added a few minutes prior to Mg^{2+} addition. The solid lines are curves generated by computer simulation, using Scheme I and the kinetic parameters listed in Table 1.